Microbial CaCO3 mineral formation and stability in an experimentally simulated high pressure saline aquifer with supercritical CO2.

Mitchell, Andrew Charles; Phillips, Adrienne J.; Schultz, Logan; Parks, Stacy; Spangler, Lee; Cunningham, Alfred B.; Gerlach, Robin

Published in:
International Journal of Greenhouse Gas Control

DOI:
10.1016/j.ijggc.2013.02.001

Publication date:
2013

Citation for published version (APA):
Mitchell, A. C., Phillips, A. J., Schultz, L., Parks, S., Spangler, L., Cunningham, A. B., & Gerlach, R. (2013). Microbial CaCO3 mineral formation and stability in an experimentally simulated high pressure saline aquifer with supercritical CO2. *International Journal of Greenhouse Gas Control*, *15*, 86-96. https://doi.org/10.1016/j.ijggc.2013.02.001

International Journal of Greenhouse Gas Control 15 (2013) 86–96

Contents lists available at SciVerse ScienceDirect

International Journal of Greenhouse Gas Control

journal homepage: www.elsevier.com/locate/ijggc

Microbial $CaCO_3$ mineral formation and stability in an experimentally simulated high pressure saline aquifer with supercritical CO_2

Andrew C. Mitchell[a,b,*], Adrienne Phillips[b,c], Logan Schultz[b,c], Stacy Parks[b,c], Lee Spangler[d], Alfred B. Cunningham[b], Robin Gerlach[b,c]

[a] Institute of Geography and Earth Sciences, Aberystwyth University, SY23 3DB, UK
[b] Center for Biofilm Engineering, Montana State University, Bozeman, MT 59717, USA
[c] Department of Chemical and Biological Engineering, Montana State University, Bozeman, MT 59717, USA
[d] Department of Chemistry and Biochemistry, Montana State University, Bozeman, MT 59717, USA

ARTICLE INFO

Article history:
Received 27 April 2012
Received in revised form
17 December 2012
Accepted 3 February 2013
Available online 6 March 2013

Keywords:
Biofilm
Calcium carbonate
Ureolysis
Supercritical CO_2
CO_2 leakage
Permeability

ABSTRACT

The use of microbiologically induced mineralization to plug pore spaces is a novel biotechnology to mitigate the potential leakage of geologically sequestered carbon dioxide from preferential leakage pathways. The bacterial hydrolysis of urea (ureolysis) which can induce calcium carbonate precipitation, via a pH increase and the production of carbonate ions, was investigated under conditions that approximate subsurface storage environments, using a unique high pressure (~7.5 MPa) moderate temperature (32 °C) flow reactor housing a synthetic porous media core. The synthetic core was inoculated with the ureolytic organism *Sporosarcina pasteurii* and pulse-flow of a urea inclusive saline growth medium was established through the core. The system was gradually pressurized to 7.5 MPa over the first 29 days. Concentrations of NH_4^+, a by-product of urea hydrolysis, increased in the flow reactor effluent over the first 20 days, and then stabilized at a maximum concentration consistent with the hydrolysis of all the available urea. pH increased over the first 6 days from 7 to 9.1, consistent with buffering by $NH_4^+ \Leftrightarrow NH_3 + H^+$. Ureolytic colony forming units were consistently detected in the reactor effluent, indicating a biofilm developed in the high pressure system and maintained viability at pressures up to 7.5 MPa. All available calcium was precipitated as calcite. Calcite precipitates were exposed to dry supercritical CO_2 ($scCO_2$), water-saturated $scCO_2$, $scCO_2$-saturated brine, and atmospheric pressure brine. Calcite precipitates were resilient to dry $scCO_2$, but suffered some mass loss in water-saturated $scCO_2$ (mass loss $17 \pm 3.6\%$ after 48 h, $36 \pm 7.5\%$ after 2 h). Observations in the presence of $scCO_2$ saturated brine were ambiguous due to an artifact associated with the depressurization of the $scCO_2$ saturated brine before sampling. The degassing of pressurized brine resulted in significant abrasion of calcite crystals and resulted in a mass loss of approximately $92 \pm 50\%$ after 48 h. However dissolution of calcite crystals in brine at atmospheric pressure, but at the pH of the $scCO_2$ saturated brine, accounted for only approximately $7.8 \pm 2.2\%$ of the mass loss over the 48 h period. These data suggest that microbially induced mineralization, with the purpose of reducing the permeability of preferential leakage pathways during the operation of GCS, can occur under high pressure $scCO_2$ injection conditions.

1. Introduction

Geologic carbon sequestration (GCS) is one strategy to reduce the emission of greenhouse gases generated through the combustion of fossil fuels. GCS involves the injection of supercritical CO_2 ($scCO_2$; critical point = 31.1 °C and 7.39 MPa) into underground formations such as depleted oil bearing formations, deep unmineable coal seams, and deep saline aquifers (White et al., 2003; Zakkour and Haines, 2007). The primary concern during the operation of GCS sites is the possibility of leakage through the injection well, other monitoring or abandoned wells and through fractures or faults in the low-permeability cap rock (Pan et al., 2009). Risk of leakage arises because $scCO_2$ is less dense and less viscous than the resident pore fluid, which allows it to migrate upward through the formation (Nicot et al., 2009).

One proposed method to mitigate leakage and enhance CO_2 storage is the use of engineered biofilms to plug porous media (Mitchell et al., 2009). Biofilms are assemblages of microorganisms, attached to surfaces, and embedded in extracellular polymeric substances (EPS). EPS is a hydrated matrix of mostly polysaccharides and proteins (Costerton and Stewart, 2001; Lewandowski

* Corresponding author at: Institute of Geography and Earth Sciences, Aberystwyth University, SY23 3DB, UK. Tel.: +44 1970 622640.
E-mail address: nem@aber.ac.uk (A.C. Mitchell).

1750-5836/$ – see front matter © 2013 Elsevier Ltd. All rights reserved.
http://dx.doi.org/10.1016/j.ijggc.2013.02.001

and Beyenal, 2007). Biofilms can reduce the permeability of porous media and have been engineered to control environmental contaminants and flow in oil reservoirs (Cunningham et al., 2003; Gerlach and Cunningham, 2010). Biofilms are the predominant way of life for most microorganisms in natural systems (Lewandowski and Beyenal, 2007). Previous experiments demonstrated that (1) *Bacillus mojavensis* biofilms can be grown in Berea sandstone cores under high pressure and $scCO_2$ injection conditions (8.9 MPa, 32 °C), (2) the biofilm can decrease the permeability of sandstone cores by approximately two orders of magnitude within a few days, (3) biofilms can resist the challenge of $scCO_2$ exposure and maintain viability with only a slight increase in permeability (Mitchell et al., 2009), and (4) biofilms formed by *B. mojavensis* exhibited only a 1 log reduction in viable cell numbers compared to a 3 log reduction for planktonic (free floating, not attached to a surface) *B. mojavensis* cells. These data demonstrate biofilm viability under high pressure and $scCO_2$ conditions relevant to GCS (Mitchell et al., 2008).

It has also been proposed that the biofilm-enhanced formation of minerals, such as calcium carbonate, can plug free pore space in porous media and result in leakage reduction (Cunningham et al., 2009, 2011; Dupraz et al., 2009; Mitchell et al., 2010). Microbially enhanced mineralization has long been recognized in modern and ancient sediments (Van Lith et al., 2003). Biofilms enhance calcium carbonate nucleation by offering negatively charged functional groups for cation adsorption and by metabolically driven changes in solution composition and pH in the biofilm microenvironment and in the bulk solution (Schultze-Lam et al., 1996). Microbially mediated urea hydrolysis is one mechanism which can enhance the formation of calcium carbonate and is being investigated for enhanced GCS (Cunningham et al., 2009, 2011; Dupraz et al., 2009; Mitchell et al., 2010). In this process, bacteria hydrolyze urea, an important nitrogen compound found in natural environments, through a series of reactions which raise the pH and alkalinity of the system through an increase in bicarbonate and carbonate concentrations. In the presence of divalent cations, such as Ca^{2+}, this increase in alkalinity can lead to the saturation and precipitation of solid calcium carbonate ($CaCO_3$).

Urea hydrolysis proceeds through a number of reactions. In the first step, urea ($CO(NH_2)_2$) is hydrolyzed to ammonia (NH_3) and carbonic acid (H_2CO_3) (Eqs. (1) and (2)) (Burne and Chen, 2000). The ammonia and carbonic acid equilibrate in water to form bicarbonate (HCO_3^-), ammonium (NH_4^+), and one hydroxide ion (OH^-) (Eqs. (3) and (4)). The increase in hydroxide ions corresponds to an increase in pH, which shifts the bicarbonate equilibrium to form carbonate ions (CO_3^{2-}) (Eq. (5)). In the presence of Ca^{2+}, $CaCO_3$ precipitation occurs (Eq. (6)) once saturation is exceeded (Burne and Chen, 2000; Castanier et al., 1999). The overall reaction summarizing the hydrolysis of urea and precipitation of $CaCO_3$ is described by Eq. (7).

$$CO(NH_2)_2 + H_2O \rightarrow NH_2COOH + NH_3 \quad (1)$$

$$NH_2COOH + H_2O \rightarrow NH_3 + H_2CO_3 \quad (2)$$

$$H_2CO_3 \leftrightarrow HCO_3^- + H^+ \quad (3)$$

$$2NH_3 + 2H_2O \leftrightarrow 2NH_4^+ + 2OH^- \quad (4)$$

$$HCO_3^- + H^+ + 2OH^- \leftrightarrow CO_3^{2-} + 2H_2O \quad (5)$$

$$CO_3^{2-} + Ca^{2+} \leftrightarrow CaCO_3 \quad (6)$$

$$CO(NH_2)_2 + 2H_2O + Ca^{2+} \leftrightarrow 2NH_4^+ + CaCO_3(\text{Overall, process}) \quad (7)$$

Other microbial metabolic processes, such as sulphate, nitrate and iron reduction could also be used to promote $CaCO_3$ formation (Van Lith et al., 2003; Van Paassen et al., 2010a), but these processes usually depend on microbial growth and cannot be controlled as easily as urea hydrolysis, which simply requires the addition of urea as a substrate, without the actual requirement of cell growth. Bacterial urea hydrolysis also does not require light, and can therefore operate in dark subsurface environments. The pH increase generated by urea hydrolysis also dramatically increases the solubility of CO_2(g), thus enhancing the rate of CO_2 solubility trapping (Mitchell et al., 2010). While there is no net mineral precipitation of CO_2 (mineral-trapping) beyond that from the urea, the mineral formed will plug subsurface pore spaces. This is particularly useful for inaccessible subsurface environments, where 'traditional' engineering approaches are not useful. For example, while injection wells may be accessible to traditional sealing approaches, such as cementing, reducing permeability proximal to the well bore or in fracture zones far from the well requires novel approaches due to the high viscosity of such traditional sealing materials. Bacteria can move through extremely small pore throat sizes of 0.4 μm < (Mitchell and Carlos Santamarina, 2004) and where pore throat size is at least twice the cell size (Jenneman et al., 1985). Since pore throat sizes in conventional reservoir rocks range from about 2 to 0.03 μm in sandstones, and from 0.1 to 0.005 μm in shales (Nelson, 2009) this demonstrates that bacteria can effectively be transported through rocks types present in common GCS sites and can likely be manipulated to grow and precipitate minerals on space and time scales by controlled injection of nutrients (Cunningham et al., 2011).

To date, ureolysis-induced $CaCO_3$ precipitation has been investigated for a number of engineering purposes including wastewater treatment (Hammes et al., 2003), soil stabilization (Harkes et al., 2010; Van Paassen et al., 2010b; Whiffin et al., 2007), immobilization of radionuclides (Mitchell and Ferris, 2005, 2006a,b; Warren et al., 2001), and mineral plugging for enhanced oil recovery and carbon sequestration (Dupraz et al., 2009; Ferris et al., 1996; Mitchell et al., 2010). All of these studies have been made at near atmospheric pressure conditions. However, in order to operate under GCS conditions, ureolytic organisms must be viable and able to hydrolyse urea under high pressure conditions (~7.5 MPa). It is also important to consider the stability of the $CaCO_3$ minerals under GCS conditions, given the potential for the dissolution of carbonate minerals in CO_2 charged acidic brine, which typically has a pH of 3.5–4 depending on brine chemistry, formation lithology, and temperature (Kaszuba and Janecky, 2009). Low pH can increase $CaCO_3$ solubility by shifting the bicarbonate equilibrium to enhance H_2CO_3 activity (Stumm and Morgan, 1996).

Here, we investigate whether ureolysis-induced $CaCO_3$ precipitation can occur under conditions that approximate subsurface storage environments, using a unique high pressure (~7.5 MPa) moderate temperature (32 °C) pulse-flow reactor system housing a synthetic porous media core. We also consider the stability of $CaCO_3$ minerals in $scCO_2$, and in likely subsurface fluids, such as brine, in the presence of and equilibrated with $scCO_2$, in order to assess the stability of biofilm formed minerals in the subsurface.

2. Experimental methods

2.1. High pressure flow reactor setup and synthetic porous media

A high-pressure flow reactor was built to investigate whether ureolysis and $CaCO_3$ precipitation in porous media could occur under high pressure conditions. The system allowed a differential pressure to be established between an input and an output high pressure accumulator, causing media to pulse-flow through a synthetic porous media core housed in a Hassler-type core holder (Temko, Tulsa, OK). The synthetic core was produced from a 2.54 cm diameter, 5 cm long high density polystyrene rod, with 6 × 1 mm internal diameter glass capillary tubes running lengthwise through the core (Supplemental Information, Fig. SI1). The capillary tubes allow the aqueous phase to pass through and microscopy to be

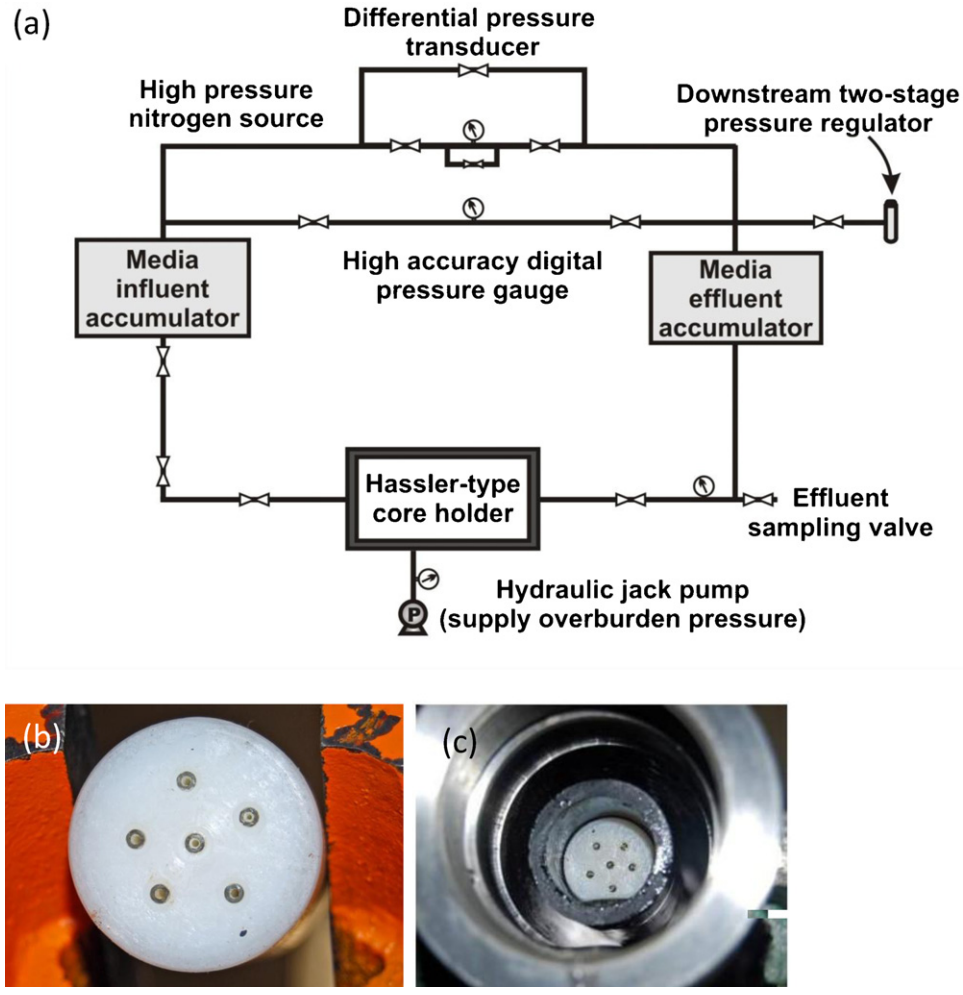

Fig. 1. (a) Schematic diagram of high pressure (~7.5 MPa) moderate temperature (32 °C) flow reactor containing synthetic porous media core. Inset pictures show (b) the synthetic porous media core with $CaCO_3$ precipitates visible on the inside of the glass tubes after an experiment, and (c) the synthetic porous media core inside the Hassler-type core holder.

performed on any biofilm and mineral precipitates formed. The high-pressure system was constructed of ¼" (6.35 mm) stainless steel tubing and Swagelok fittings housed in an incubator to control temperature at 32 ± 0.2 °C. The media reservoirs were water service piston-type accumulators (Parker, Inc.) designed to withstand pressures of 21 MPa (Fig. 1).

Prior to loading the synthetic core, the input media accumulator and influent tubing were sterilized by exposure to 10% bleach in 6 g L^{-1} TWEEN 80 solution, followed by 2.25 g L^{-1} sodium thiosulphate solution, followed by a 70% ethanol solution (Barkley and Richardson, 1994). Next, the synthetic core was loaded into a Buna-N (TEMCO) sleeve and the core holder was reassembled. The core and core sleeve were not sterilized by autoclaving nor chemical treatment. The annulus of the core holder was filled with water and an overburden pressure of about 10.5 MPa was provided by a hydraulic jack pump. The core holder and media accumulators were connected to the high-pressure flow system which was housed in an incubator at 32 ± 0.2 °C (Fig. 1).

2.2. Flow reactor inoculation and operation

Sporosarcina pasteurii (ATCC 11859, gram-positive, spore-forming, urease positive), known to induce $CaCO_3$ precipitation in the presence of urea and dissolved Ca (Fujita et al., 2008; Mitchell and Ferris, 2005, 2006b) was used for the experiments. *S. pasteurii* was grown to the exponential growth phase, prior to inoculating the high pressure system containing the synthetic core, in filter sterilized $CaCO_3$ mineralizing medium (CMM) described by Ferris et al. (1996) which contained 3 g L^{-1} Nutrient Broth, 333 mM Urea, 187 mM NH_4Cl, 25 mM $NaHCO_3$, and was pH adjusted to 6 with concentrated HCl. The CMM excluded calcium for preparation of the *S. pasteurii* inoculum and flow reactor inoculation (CMM−) but 25.2 mM $CaCl_2 \bullet 2H_2O$ was included during the main precipitation experiment (CMM+). To inoculate the core, it was isolated and ~40 ml of the exponential growth phase culture of *S. pasteurii* was injected using a 60 ml sterile syringe attached to a Swagelok fitting tightened onto the influent side of the core holder. The inoculum remained in the core for 16 h and then sterile CMM− was pumped through the core at atmospheric pressure using a peristaltic pump at 8.86 ml h^{-1} for 16 days. The use of a rich growth medium and urea allowed *S. pasteurii* biofilm to develop on the internal surfaces of the core and for ureolysis to occur. On day 17, the media accumulator was filled with 1100 ml of sterile CMM− solution using a peristaltic pump and N_2 gas was used to pressurize the system to 1.43 MPa, with a differential pressure across the core of 0.1 MPa (Fig. 1). After being allowed to acclimatize to the system temperature, sterile CMM− was pulsed into the core, induced by the constant differential pressure across the core. After 24 h, the media in the core was collected in the output media accumulator. Sterile CMM− was then pulsed into the core again from the input media accumulator. For the next 20 days, fresh sterile CMM− was pulsed daily into the core, and medium that had resided

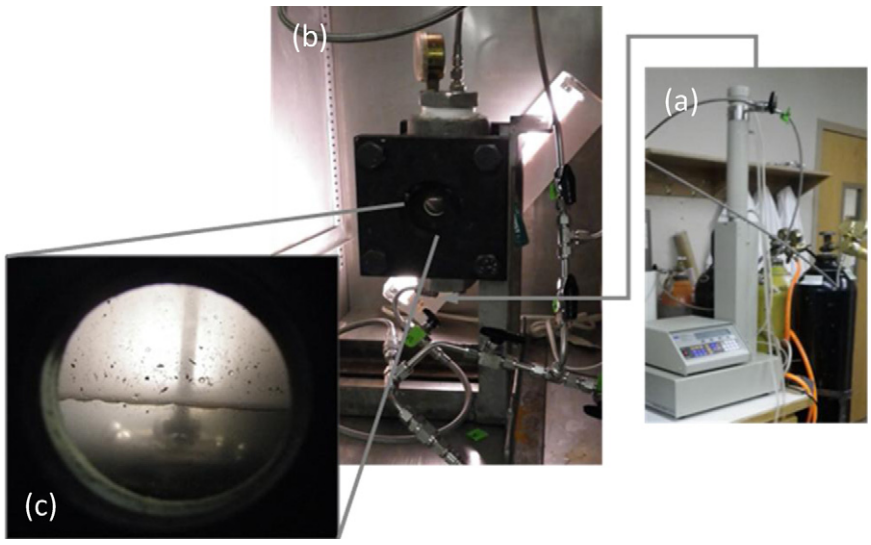

Fig. 2. Pictures of the high pressure vessel (HPV) used to challenge $CaCO_3$ precipitates with $scCO_2$ and brine. HPV was also used to incubate Ca free mineralizing medium (CMM−) described by Ferris et al. (1996) and Ca inclusive CMM (CMM+) abiotically at 7.5 MPa in the absence of $scCO_2$ to demonstrate that no abiotic hydrolysis of urea occurred at the high pressures used in this study. (a) Supercritical CO_2 is pumped by a Teledyne Isco (Lincoln, Nebraska) pump into the (b) view-ported HP(c) the view port image of the HPV shows $scCO_2$ in the headspace and $scCO_2$ saturated brine in the bottom of the HPV during an exposure (see also Video 1).

in the core for 24 h was collected in the effluent. During this 20-day period, system pressure was gradually increased from 1.43 MPa to 7.5 MPa ± 0.1% while maintaining a differential pressure across the core between 0.1 and 0.55 MPa ± 0.1%. On day 39, the input media accumulator was filled with CMM+, and the same daily pulsing procedure was continued, in order to induce $CaCO_3$ precipitation. Effluent from the flow reactor was collected daily and analyzed for pH, NH_4^+, Ca^{2+} and ureolytic cell counts, as described in Section 2.3. This procedure was performed in order to elucidate whether *S. pasteurii* viability could be maintained and ureolysis could occur at pressures at which $scCO_2$ could be present. During the experiment, CMM− and subsequently CMM+ were sampled from the input media accumulator in order to check for bacterial contamination, as described below. Control experiments were also performed to check ureolysis could not occur abiotically under pressure, by pressurizing CMM− and CMM+ to 7.5 MPa in a separate high pressure vessel (HPV) (Fig. 2) in the absence of *S. pasteurii*.

2.3. Flow reactor effluent analysis

Effluent that had resided in the core for 24 h and had then been pulsed out of the core was collected from the output media accumulator and immediately filter sterilized through 0.2 μm polycarbonate membranes and tested for pH using a Fisher Scientific (Fair Lawn, NJ) pH/ion/conductivity meter. The meter was calibrated daily using pH 7 and pH 10 buffer solutions (Fisher Scientific). Ammonium concentrations were determined using the Nessler Assay (Mitchell and Ferris, 2005) by comparing sample results to standards made with NH_4Cl. Ca^{2+} concentrations were determined using an Agilent 7500ce Inductively Coupled Plasma Mass Spectrometer (ICP–MS) in Montana State University's Environmental and Biofilm Mass Spectrometry Facility. Non-filtered effluent was used to determine the number of ureolytic colony forming units (CFUs) as a measure of ureolytic cell viability on a daily basis. Effluent was serially diluted in Phosphate Buffered Saline solution, from 10^{-1} to 10^{-5} and plated onto agar plates, supplemented with 37 g L^{-1} Brain Heart Infusion, and 20 g L^{-1} urea. 30 randomly selected CFUs were individually picked and grown in individual wells containing 250 μL of BHI + 20 g L^{-1} urea solution in a 96 well plate. Plates were incubated at 30 °C for 24 h, and individual wells were tested for ammonium using the Nessler Assay to confirm ureolytic activity (Mitchell and Ferris, 2005). CFU's and pH were also measured from the influent CMM− and subsequently CMM+, in order to check for ureolytic bacteria contamination. Further details are given in the Supplemental Information, Section SI1. The glass capillary tubes running lengthwise through the synthetic core were removed and imaged on a Nikon SMZ1500 stereoscope.

2.4. Calcium carbonate brine and supercritical CO_2 challenges

In order to test the stability of ureolysis-induced $CaCO_3$ precipitates under high pressure $scCO_2$ conditions relevant to subsurface storage sites, $CaCO_3$ was challenged with supercritical CO_2 ($scCO_2$), $scCO_2$ saturated brine (brine co-equilibrated with $scCO_2$), brine-saturated $scCO_2$, and atmospheric pressure brine at two different pH values (pH 7.61 and 4, Table 1). Pyrex bottles containing pre-weighed black polycarbonate coupons and containing 250 ml CMM+ were inoculated with 1 ml of *S. pasteurii* in the exponential growth phase, and incubated at 30 °C to induce ureolysis and $CaCO_3$ precipitation onto the coupons. Coupons were also incubated in sterile, uninoculated CMM+ medium to confirm abiotic precipitation was not occurring. Black polycarbonate was used to provide contrast with the precipitated $CaCO_3$ for light microscopy. After 24–48 h of incubation and precipitation, coupons were removed with sterilized tweezers and dried for more than 24 h at 65 °C until constant weight was achieved. Mineral not firmly attached to the coupon was gently blown off the coupon using compressed air (Falcon Dust Off, Branchburg, NJ). The coupons were weighed again periodically over a period of 24 h to confirm constant weight before they were imaged on a Nikon SMZ 1500 stereoscope (Supplemental Information, Section SI2). Coupons were then challenged with $scCO_2$, $scCO_2$ saturated brine, brine saturated $scCO_2$ and atmospheric pressure brine, as described below.

2.4.1. Atmospheric pressure brine

Synthetic NaCl rich brine of a 162 g L^{-1} TDS (1.5 M strength, used by Kaszuba et al., 2003), containing 683 mM NaCl, 16.4 mM $MgSO_4 \bullet 7H_2O$, 5.5 mM $CaCl_2 \bullet 2H_2O$, 480 mM $MgCl_2 \bullet 6H_2O$, 264 mM KCl, and 1.79 mM KBr, with a resulting pH of 7.61 was prepared and filter sterilized. Mineral-covered coupons were placed in the synthetic brine for 4 h, 24 h, and 168 h (Exposures 1–3, Table 1). After

Table 1
Summary of $scCO_2$ and/or brine exposures of $CaCO_3$ undertaken in the high pressure vessel.

Exposure	Pressure	Temperature	Description
1	Ambient	Room	Coupons in brine for 4 h, initial pH 7.61
2	Ambient	Room	Coupons in brine for 24 h, initial pH 7.61
3	Ambient	Room	Coupons in brine for 168 h, initial pH 7.61
4	1300 psi	37 °C	Coupons in $scCO_2$ for 2 h
5	1250 psi	37 °C	Coupons in brine-saturated $scCO_2$ for 2 h
6	1250 psi	37 °C	Coupons in brine-saturated $scCO_2$ for 48 h
7	1250 psi	37 °C	Coupons in $scCO_2$-saturated brine for 2 h
8	1250 psi	37 °C	Coupons in $scCO_2$-saturated brine for 48 h
9	Ambient	Room	Coupons in pH 4 brine for 2 h
10	Ambient	Room	Coupons in pH 4 brine for 48 h
11	Ambient	Room	Sterile control

removal from the brine, coupons were rinsed in DI water to remove residual brine and then dried, weighed, and imaged, as described above.

2.4.2. Supercritical CO_2 ($scCO_2$)

Coupons were loaded into the HPV system (Fig. 2). The system was pressurized and $scCO_2$ was pumped under constant flow via a Teledyne Isco high pressure pump to the HPV until pressure stabilized at 8.9 MPa. Pressure and temperature were maintained at 8.9 ± 0.4 MPa and 37 ± 0.2 °C, respectively (Exposure 4, Table 1), well above that required for supercritical conditions to account for the accuracy of the pressure and temperature gauges. The system was depressurised after 2 h, and immediately the coupons were removed from the reactor, rinsed, imaged with the stereoscope, dried and weighed, as described above.

2.4.3. $ScCO_2$ saturated brine and brine saturated $scCO_2$

350 ml of brine was added under ambient pressure conditions into the HPV. Coupons were placed into the reactor so three coupons were wetted in the brine (bottom portion of reactor) and three were in the headspace of the reactor. The system was pressurized and $scCO_2$ was pumped into the HPV and bubbled through the brine until pressure in the reactor stabilized at 8.9 ± 0.4 MPa at 37 ± 0.2 °C. The increase in surface area between the CO_2 bubbles and the brine as well as the resulting mixing are assumed to have resulted in sufficient mass transfer to produce $scCO_2$ saturated brine and brine saturated $scCO_2$ in the lower and upper portions of the HPV, respectively. Hence, the coupons in the HPV were exposed to brine saturated $scCO_2$ (in the headspace portion) and supercritical CO_2 saturated brine (bottom portion of the reactor) at 8.9 MPa and 37 °C for 2 h and 48 h (exposures 5 and 7, and 6 and 8 respectively, Table 1). Immediately after each exposure, the coupons were removed from the HPV, rinsed in DI water to remove any residual brine, imaged with the stereoscope, dried and weighed, as described above.

Experiments were also performed in order to separately investigate the effect of pH on mineral mass loss by exposing mineralized coupons to pH adjusted brines at atmospheric pressure. Isolating the effect of pH was necessary because during depressurisation and CO_2 degassing of the HPV, extreme physical agitation of the brine occurred which may have accounted for mineral mass loss, and this would not be representative of processes that would occur under GCS field conditions. In order to estimate the pH of the $scCO_2$ saturated brine used in the current study, pH was measured in $scCO_2$ saturated brines in a similar high pressure flow system at MSU, equipped with an in-line Barben Analyzer Technology pH probe connected to a Campbell Scientific CR1000 data logger. The observed pH was 3 in a 0.5 g L^{-1} TDS brine and 4 in a 5 g L^{-1} TDS brine (Hansen, 2009), consistent with the decreased solubility of CO_2 in higher salinity solutions (Duan and Sun, 2003; Lagneau et al., 2005). These observations agree with reports by (Kaszuba and Janecky, 2009) who report typical pH values of 3.5–4 for CO_2 charged acidic brines. Therefore the pH of the 162 g L^{-1} TDS brine used in the current study was estimated to have a pH of > 4. Hence, in order to expose the coupons to the most acidic conditions likely, brine was adjusted to pH 4 with HNO_3, and coupons were exposed to this brine for varying lengths of time. Large volume-to-carbonate mineral ratios were used to minimize pH changes due to $CaCO_3$ dissolution and maintain the pH at 4. Minerals from each of the experiments were examined with XRD to determine the mineralogy of the precipitates before and after exposure (Supplemental Information, Section SI2).

3. Results

3.1. Ureolysis and carbonate mineral formation at ~7.5 MPa pulse-flow conditions

The flow reactor was operated at atmospheric pulse-flow conditions with calcium free medium (CMM−), for the first 17 days of the experiment. During this period, NH_4^+ concentrations increased gradually from ~3000 mg L^{-1}, which is the free NH_4^+ concentration in the CMM− from NH_4Cl, to ~11,000 mg L^{-1}, indicating the liberation of NH_4^+ from the hydrolysis of urea (Eqs. (1), (2) and (4)) (Fig. 3). The pH also increased from 7 to 9.1 within the first 5 days (Fig. 3), consistent with buffering by $NH_4^+ = NH_3 + H^+$, the dominant buffer in the system, which has a pK_a value of 9.3 at 30 °C (Mitchell and Ferris, 2005). Viable cells measured in the reactor effluent generally increased during this period, up to a maximum of $5.2 \pm 1.1 \times 10^7$ CFU, and 100% of the tested CFUs were ureolytically active (Fig. 3). Influent media samples during this period exhibited NH_4^+ concentrations of ~3000 mg L^{-1}, a pH of ~7, and there were no detectable CFUs (Fig. 3), demonstrating that the influent medium had not been contaminated by ureolytic organisms, and that ureolysis was occurring only in or downstream of the synthetic porous media core.

Starting on day 18, pressure was gradually increased from atmospheric to 7.5 MPa as the daily pulse-flow of CMM− continued (Fig. 3). During this period, effluent pH remained at ~9.1. NH_4^+ concentrations gradually increased over this period to a maximum of $14{,}600 \pm 1229$ mg L^{-1}, consistent with the hydrolysis of all the available urea, as did ureolytic CFUs, on average which increased to $2.1 \times 10^7 \pm 4.8 \times 10^6$ (Fig. 3). During the period of pressurization ~7.5 MPa, influent media still exhibited NH_4^+ concentrations of ~3000 mg L^{-1}, pH was ~7, and there were no CFUs, again indicating that the influent medium had not been contaminated by ureolytic organisms, and that ureolysis was occurring in the synthetic porous media core (Fig. 3). Pressurization of the CMM− and the calcium inclusive media, CMM+, in the absence of *S. pasteurii* to 7.5 MPa in the HPV for 24 h (Fig. 2) did not result in any NH_4^+ production, change in pH or, in the case of the CMM+ experiments,

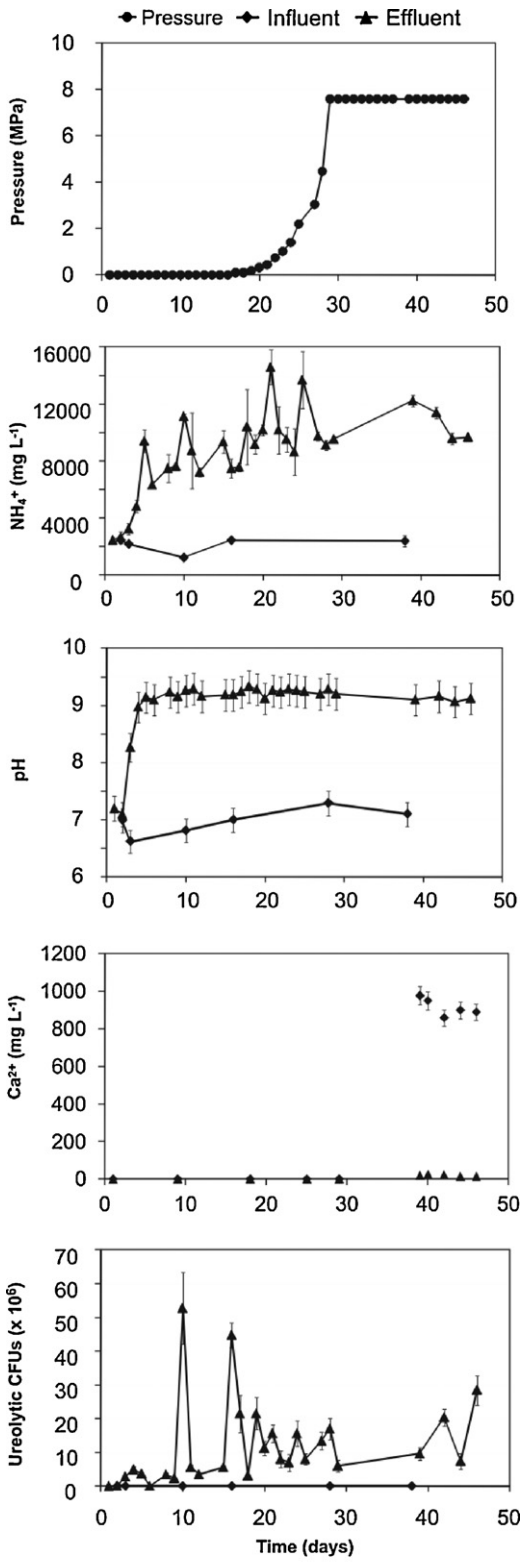

Fig. 3. Pressure, influent and effluent NH_4^+, pH, Ca^{2+} and ureolytic colony forming units from the high pressure (~7.5 MPa) moderate temperature (32 °C) flow reactor containing a synthetic porous media core. Ca free $CaCO_3$ mineralizing medium (CMM−) described by Ferris et al. (1996) was used as the influent media from time 0 to day 38, after which the CMM media included Ca (CMM+).

Table 2
Aqueous chemistry of $CaCO_3$ mineralizing medium (CMM+) described by Ferris et al. (1996) after exposure to abiotic high pressure conditions (8.9 MPa) in the high pressure vessel. Experiments repeated with CMM excluding calcium (CMM−) demonstrating that urea hydrolysis is not induced abiotically by high pressure conditions. Concentrations in mg L^{-1}.

Sample	pH	NH_4^+	Na^+	Mg^{2+}	K^+	Ca^{2+}	Ba^{2+}
CMM− + pressure	7.37	3.22	6.76	0.025	1.15	0.200	0.001
CMM−	7.15	3.45	6.60	0.025	1.12	0.18	0.001
CMM+ + pressure	7.31	2.95	6.48	0.025	1.11	9.71	0.001
CMM+	7.25	2.35	6.49	0.025	1.06	9.20	0.001

decrease in Ca^{2+} concentrations, which confirmed that increased pressure alone did not result in the hydrolysis of urea (Table 2).

After the flow system had been pressurized to 7.5 MPa, the influent was switched to CMM+, containing 1000 mg L^{-1} (25 mM) Ca^{2+}. The concentration of Ca^{2+} in the flow reactor effluent was only 12 ± 0.6 mg L^{-1} after the first 24 h, and remained at this concentration for the remainder of the experiment (Fig. 3). During this period, there were no appreciable changes in effluent pH, NH_4^+ concentrations, or ureolytic CFUs. After 45 days the system was depressurised and the glass capillaries inside the core were retrieved. Stereoscope (Fig. 4) and XRD analysis (Supplemental Information, Fig. SI2) indicated that calcite had precipitated inside the glass capillaries of the core, demonstrating that ureolysis induced $CaCO_3$ precipitation occurred under high pressure conditions ~7.5 MPa. Additionally, no precipitates were observed in the effluent accumulator, and the influent CMM+ media exhibited consistent Ca^{2+} concentrations of ~1000 mg L^{-1}, indicating that precipitation occurred in the core region under pressure or down the flow path of the core (Fig. 3), and not in the effluent accumulator during depressurisation. A crystal density gradient could be observed, with a greater crystal density in the up flow (influent) end of the core. Crystal size analysis with ImageJ software (Mitchell and Ferris, 2006a,b) of 5 stereoscope images from throughout the core revealed the average, minimum and maximum crystal size was 57 μm, 10 μm and 102 μm respectively, with a standard deviation of 21 μm. This ignored crystals below the stereoscope detection limit of ~5 μm (Schultz et al., 2011).

3.2. Calcium carbonate mineral stability with supercritical CO_2/brine mixtures

In order to examine stability of the microbiologically precipitated $CaCO_3$ during brine and $scCO_2$ exposure, $CaCO_3$ precipitates on polycarbonate coupons were challenged with $scCO_2$-brine mixtures at high pressure (~8.9 MPa) conditions in the HPV (Fig. 5) and also atmospheric pressure brines. Incubation of $CaCO_3$ in brine, pH 7.61, at atmospheric pressure for 4 h, 24 h and 1 week, lead to a $CaCO_3$ mass change of $-7 \pm 0.036\%$, $-10\% \pm 4.7\%$ and $-23\% \pm 2.5\%$ respectively for experiments 1–3. However the difference in mineral mass from before and after exposure was not statistically significant for the three experiments (Fig. 5) and therefore did not suggest that brine exposure at atmospheric conditions led to a statistically significant change in the mass of $CaCO_3$ on these timescales. Exposure to $scCO_2$ for 48 h did not lead to an observable mass change ($-0.4 \pm 0.01\%$ variation) demonstrating that dry (i.e. not moisture containing) $scCO_2$ has no effect on the mineral mass. The exposure of $CaCO_3$ to brine saturated with $scCO_2$ resulted in a significant mass change of $CaCO_3$ during both 2 h (-84%, $\pm 35\%$ variation) and 48 h (-92%, $\pm 50\%$ variation) of exposure. However, this mass loss is being attributed to an artifact associated with the depressurization process, which resulted in significant turbulence in the brine filled portion of the HPV. Highly intense bubble formation was observed during out-gassing of CO_2 during depressurization, which occurred at a rate of 1.158 MPa min^{-1} for the 2 h

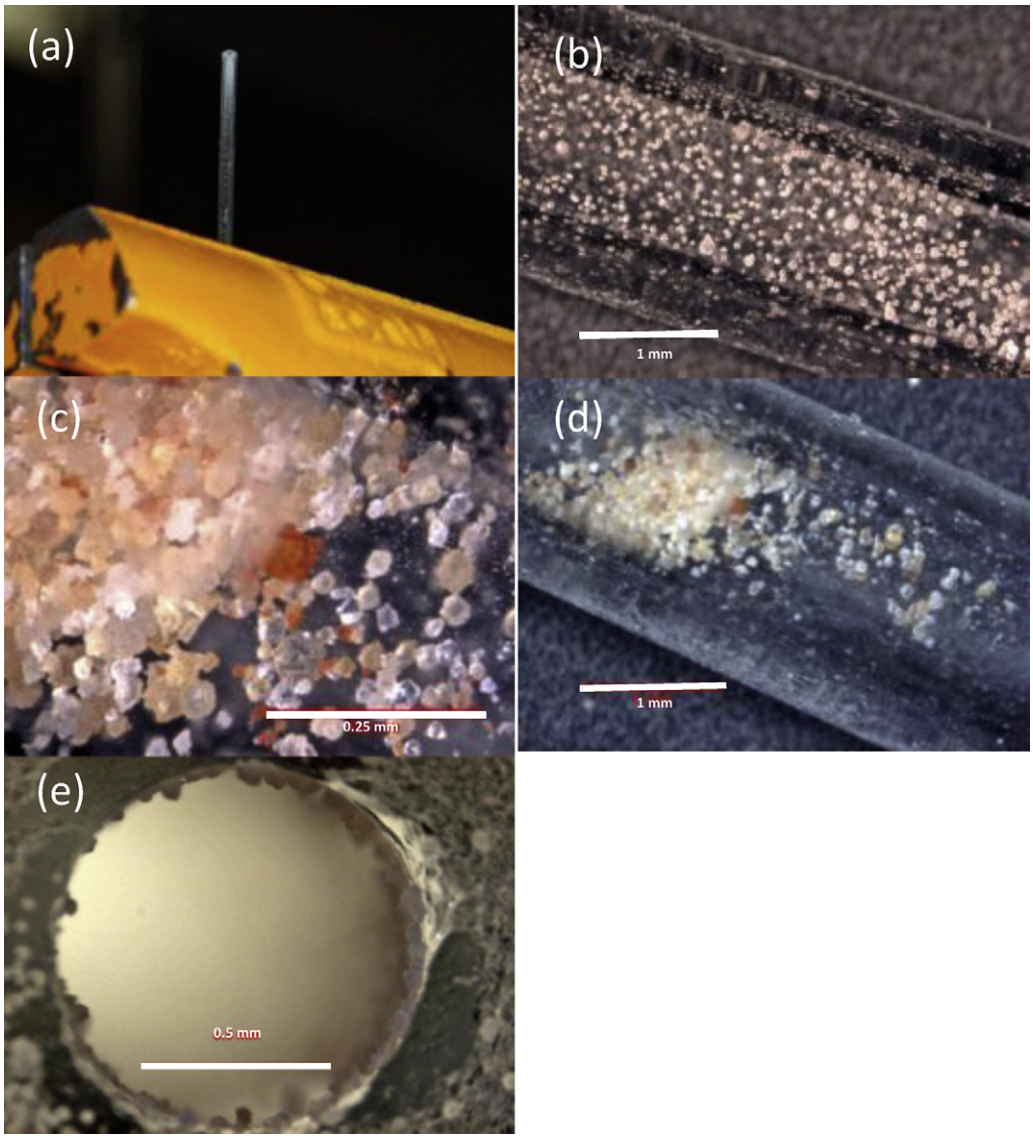

Fig. 4. Images of $CaCO_3$ precipitates formed inside the capillary of the synthetic porous media core in the high pressure (~7.5 MPa) moderate temperature (32 °C) flow reactor. (a) $CaCO_3$ precipitates (in white) inside one of the 5 cm long glass tubes (capillaries) that were inserted in the artificial core. Decreasing crystal density can be seen in the direction of flow (top is influent, bottom effluent). (b–e) Stereoscope images: (b) small $CaCO_3$ crystals inside the 1 mm internal diameter capillary, (c and d) close-up images of a cluster of $CaCO_3$ crystals, (e) view into capillary from influent end showing $CaCO_3$ coating on the inside wall of the capillary. While crystals were clearly visible, no extensive EPS rich biofilm was observed.

exposure and 3.08 MPa min^{-1} for the 48 h exposure. The resulting turbulence, clearly visible through the sight glass (Video 1), is believed to have mechanically abraded $CaCO_3$ from the coupons, as evidenced by the discovery of some $CaCO_3$ crystals in the bottom sump of the HPV. $CaCO_3$ minerals in the headspace of the HPV, above the $scCO_2$ saturated brine (i.e. exposed to $scCO_2$ saturated with brine vapour) exhibited a mass change of $-36 \pm 7.5\%$ during 2 h of exposure, and $-17 \pm 3.6\%$ during 48 h of exposure.

Due to the physical disturbance that the coupons undergo during depressurisation and degassing of the brine, and the effect this could have upon the mineral mass loss, coupons were also exposed to brine at atmospheric pressure, acidified to pH 4, the estimated pH of the 1.5 M $scCO_2$ saturated brine at 8.9 MPa used in the $scCO_2$ saturated brine experiments (Allen et al., 2005; Carey et al., 2010; Duan and Sun, 2003; Kaszuba and Janecky, 2009; Kaszuba et al., 2003, 2005; Lagneau et al., 2005), in order to determine mineral dissolution associated with low pH conditions alone. This revealed a small mass change of only $-3.4 \pm 0.67\%$ over 2 h and $-7.8 \pm 2.2\%$ over 48 h (Fig. 5). Stereoscope images of the $CaCO_3$ precipitates before and after exposure to the $scCO_2$-brine mixtures exhibited no major morphological changes on the 10–100 μm scale (Fig. 6). XRD analysis of the precipitates before and after the $scCO_2$/brine mixtures revealed only calcite, demonstrating that there were no changes in mineralogy due to interaction with $scCO_2$ and brine (Supplemental Information, Section SI2, Fig. SI2).

4. Discussion

4.1. Ureolysis and carbonate mineral formation at ~7.5 MPa pulse-flow conditions

The use of a unique high pressure, moderate temperature pulse-flow system has demonstrated that bacterial urea hydrolysis by *S. pasteurii* and associated $CaCO_3$ precipitation can occur under pressure conditions that approximate subsurface CO_2 storage environments. These observations are consistent with previous studies of *S. pasteurii* at atmospheric pressure, demonstrating the organism's ureolytic capability (Ferris et al., 2003; Fujita et al.,

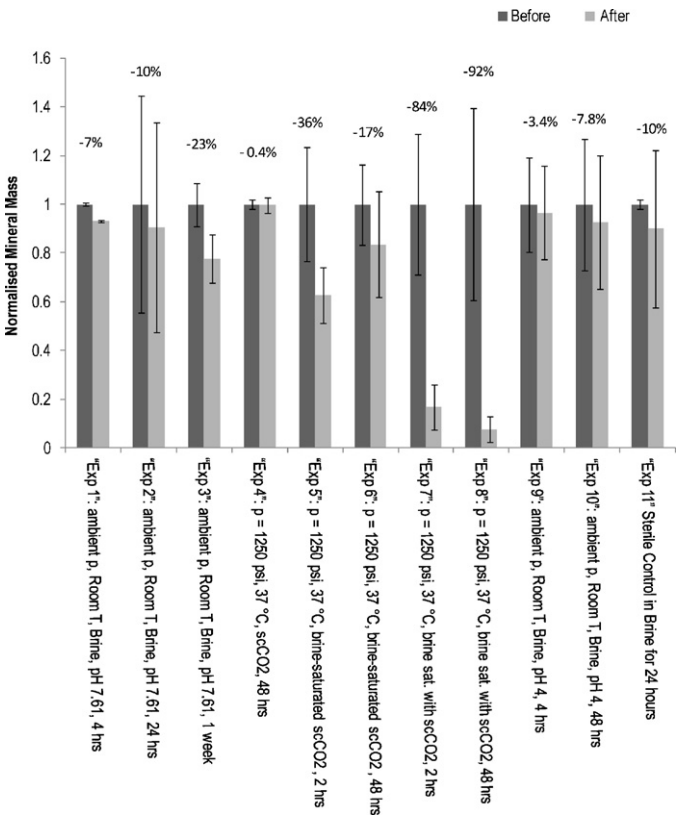

Fig. 5. Change in mass of $CaCO_3$ on coupons (normalized to initial mineral mass) before and after challenges in the high pressure vessel (HPV) (see Table 1) with percentage change of mass listed. Three or more coupons used in each experiment.

2000; Warren et al., 2001). High pressures have previously been reported to significantly affect the metabolic functions and growth of mesophilic organisms, such as *S. pasteurii*, by inhibiting DNA replication and protein synthesis (Abe et al., 1999; Gross et al., 1993; Yayanos and Pollard, 1969). However, ureolytic CFUs up to $5.2 \pm 1.1 \times 10^7$ CFU/mL in the reactor effluent indicate that *S. pasteurii* maintained viability under conditions of approximately 7.5 MPa, demonstrating that elevated pressures did not fatally inhibit cell function.

Ureolytic CFUs in the reactor effluent were, on average, higher during the period of pressurization at 7.5 MPa (day 18 onwards), when NH_4^+ concentrations were also at their maximum of $14{,}500 \pm 1200$ mg L^{-1}, a concentration which was consistent with the hydrolysis of all the available urea in the influent media. This suggests that ureolytic biomass increased during the course of the experiment and indicates that during the period of pressurization at 7.5 MPa, ureolysis was limited by the mass transport of urea, rather than available ureolytic biomass, under pulse-flow conditions in the synthetic porous media core. In contrast, prior to pressurization, while biomass was increasing in the core, as indicated by increasing CFUs in this period, ureolysis was likely limited by the available ureolytic biomass rather than reactant supply until approximately 17 days, since NH_4^+ concentrations were less than could be produced by the available urea, at only ~11,000 mg L^{-1}.

The high pressure flow system was only inoculated once at the beginning of the experiment, yet significant numbers of viable ureolytic cells were observed in the effluent over the course of the experiment. Therefore, it appears a well established surface-associated community, or biofilm, developed in the high pressure system. Previous studies at atmospheric pressures have demonstrated that *S. pasteurii* can be effectively distributed and attached to porous media surfaces, including sand beds (Harkes et al., 2010; Van Paassen et al., 2010b), and glass capillaries (Schultz et al., 2011). In these studies, media flow was induced that allowed a surface-associated community to develop after initial inoculation.

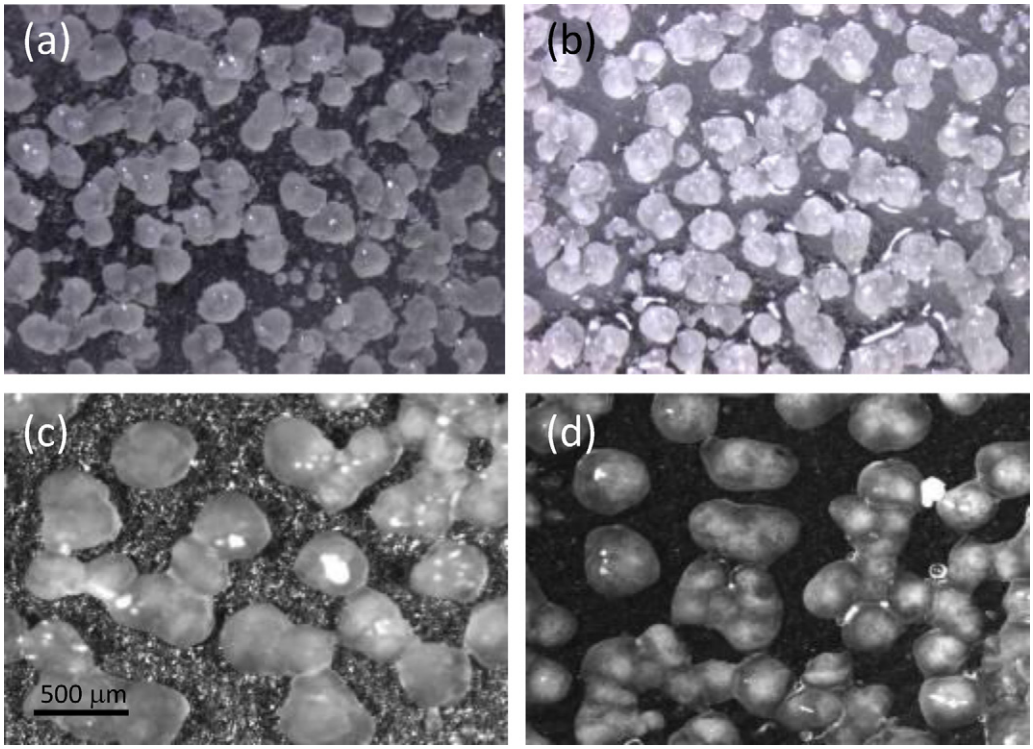

Fig. 6. Stereoscope images of coupons exposed brine and $scCO_2$ before (a and c) and after (b and d) challenge in the high pressure vessel (HPV). Images are at 40× magnification. No major morphological changes to $CaCO_3$ crystals noticeable on this scale.

Schultz et al. (2011) demonstrated using confocal laser scanning microscopy, that the surface associated *S. pasteurii* did not form extensive EPS, but rather a discrete cell coverage on the capillary surface and calcite surfaces, which supports observations made in this study where only $CaCO_3$ crystals but no EPS was observable under high pressure pulse-flow conditions (Fig. 4). The low pH and NH_4^+ concentration in the influent media accumulator demonstrates the biofilm community must have been present only in the synthetic porous media core or downstream of the core. Biofilms are often more resilient to physical chemical, and biological stresses than free floating, or planktonic cells, of the same organism (Costerton and Stewart, 2001; Lewandowski and Beyenal, 2007; Stewart, 2003). Indeed, it was previously demonstrated by us that planktonic *B. mojavensis* cultures exposed to flowing $scCO_2$ at 136 atm and 35 °C for 19 min lead to a 1000-fold reduction in viable cell numbers, while biofilm cultures only showed a 10-fold reduction in viable cell numbers (Mitchell et al., 2008). These data suggest that the biofilm state of *S. pasteurii* in the porous media core in the high pressure system may have promoted growth and function under high pressure conditions compared to the planktonic form.

The flow system demonstrates ureolysis-induced $CaCO_3$ precipitation can occur under high pressure conditions. This would be expected under the high pH conditions maintained under pressure by ureolysis, which shifts the bicarbonate equilibrium to form carbonate ions (CO_3^{2-}) which, in the presence of Ca^{2+}, precipitates out of solution as $CaCO_3$ if the solubility product for calcite is exceeded (Burne and Chen, 2000; Castanier et al., 1999). Indeed, in the high pressure flow reactor experiments, pH measured in the depressurized effluent fluids (Fig. 3) will represent the in situ pH under high pressure conditions because nitrogen gas and not CO_2 was used for pressurization. If a separate CO_2 phase had been present at elevated pressures, degassing of CO_2 from the reactor effluent would have resulted in a shift of the carbonate speciation in solution, leading to an increase in pH relative to the in situ (high pressure) conditions. This could have resulted in the precipitation of $CaCO_3$ during depressurization (Murray et al., 1980; Stumm and Morgan, 1996). However, the precipitation of $CaCO_3$ during depressurization is unlikely to have occurred since N_2 was the overburden gas and outgassing of CO_2 was likely not a significant factor. The lack of $CaCO_3$ precipitates in the effluent accumulator confirms $CaCO_3$ precipitation occurred in the core region before the accumulator, and must have been caused by ureolysis induced pH and carbonate ion concentration increases. Pressure increases the solubility of $CaCO_3$, and thus the ion activity product at saturation (Pytkowicz and Conners, 1964). In artificial seawater at 10 MPa, the ion activity product at saturation is 1.093 times greater than at atmospheric pressure (Pytkowicz and Conners, 1964), demonstrating that under fixed Ca concentrations, slightly more urea would be hydrolysed before $CaCO_3$ saturation is reached than at atmospheric conditions. Saturation index (SI) modeling on PHREEQCi (Parkhust and Appelo, 1999) with analysis of the media under standard conditions (1 atm and 25 °C) demonstrates that saturation is reached [$SI = \log(\{Ca^{2+}\}\{CO_3^-\}/K_{sp}) = 0$] when only 1.05 mM urea has been hydrolysed. This suggests at the maximum pressure of 7.5 MPa used the experiments, 1.15 mM of urea was hydrolysed before $CaCO_3$ precipitation was induced. However, this will be a minimum value, as supersaturation is often required before precipitation is initiated because the nucleation activation (i.e., interfacial) free energy barrier has been surmounted (Stumm and Morgan, 1996). Indeed, in abiotic $CaCO_3$ precipitation experiments, 2D heterogeneous nucleation on seed particles has been observed at a minimum SI of 0.78 (Teng et al., 2000), and spontaneous 3D homogeneous nucleation in unseeded solutions has been observed at SIs of 1.83–1.99 (Gómez-Morales et al., 1996). In the high pressure flow system, calcite precipitation would be likely be initiated by a combination of 3D homogenous nucleation in solution and 2D heterogeneous nucleation on the capillary walls, nascent crystals, and bacterial cell surfaces (Ferris et al., 2003; Fujita et al., 2000; Mitchell and Ferris, 2005, 2006b). Crystals were observed attached to the capillary walls (Fig. 4b, e and f), as well as agglomerates of loose crystals forming plugs (Fig. 4c and d) suggesting multiple mechanisms of nucleation and growth.

Experimental and modeling studies demonstrate that during ureolysis, the highest pH, concentrations of carbonate ions, and thus saturation, will occur proximal to, and decrease away from cells (Mitchell and Ferris, 2006b; Zhang and Klapper, 2010), suggesting 2D *nucleation* in the flow system will preferentially occur near cells. However, the decrease in crystal size densities in the capillary along the flow direction of the core (Fig. 4a) suggests that crystal *growth* was controlled by reactant supply and nuclei grew faster in the inlet region, where reactants, and thus precipitation rates are higher due to the increased SI and availability of higher Ca^{2+} and CO_3^{2-} concentrations (Ferris et al., 2003; Mitchell and Ferris, 2005; Teng et al., 2000). Crystal sizes were much larger (average = 57 μm) than previously observed for ureolysis induced $CaCO_3$ precipitation (~1–6 μm) (Mitchell and Ferris, 2006a,b). This primarily reflects a higher total reactant supply provided by pulse-flow operation of the high pressure experiments (20.16 mg Ca^{2+} and 433 mg CO_3^{2-} over the 9 days of CMM+), compared to previous batch experiments [5.25–17.5 mg Ca and 79–264 mg CO_3^{2-} (Mitchell and Ferris, 2006a,b)] (Supplemental Information, Section SI3). Nevertheless at the termination of the high pressure pulse-flow experiment, plugging had not occurred due to the relatively limited supply of reactants compared to the pore space in the synthetic core, calculated as 0.0185 cm^3 $CaCO_3$ relative to 0.196 cm^3 void space in the synthetic porous media core (Supplemental Information, Section SI4). However, permeability reduction and plugging would have occurred given the supply of sufficient reactants, as demonstrated for ureolysis-induced $CaCO_3$ precipitation in atmospheric pressure constant-flow systems (Cunningham et al., 2011; Schultz et al., 2011).

4.2. Calcium carbonate mineral stability with supercritical CO_2/brine mixtures

The significant mass change observed in the $scCO_2$ saturated brine challenges over 2 h (−84 ± 35% mass loss) and 48 h (−92 ± 50% mass loss) appeared to reflect physical dislodging of the $CaCO_3$ crystals from the coupon surface, particularly during the depressurisation of the HPV which caused violent bubbling when CO_2 was degassing from the brine (Video 1). This was supported by the small mass change of $CaCO_3$ in atmospheric pressure brine at pH 4, the estimated pH of the $scCO_2$ saturated brine (−3.4 ± 0.67% over 2 h, −7.8 ± 2.2% over 48 h). This minor mass change of $CaCO_3$ demonstrated that acidity-driven dissolution of $CaCO_3$ was negligible. $CaCO_3$ dissolution in the $scCO_2$ saturated brine driven by low pH has been observed in other studies of acidic brine–$CaCO_3$ interactions (Carey et al., 2010; Gledhill and Morse, 2004, 2006; Sanz et al., 2011) and would be expected under the experimental conditions used here. The apparent lack of this phenomenon could be firstly due to mass transport limitations in the static brine–$CaCO_3$ mixture in the HPV, where reaction kinetics are reduced by the limited ability of reactants (e.g. H^+) to reach the mineral surface and products (Ca^{2+} and CO_3^{2-}) to migrate away from the mineral surface by advection. Indeed, at low pH values, the kinetics of calcite dissolution are controlled by mass transport because surface controlled processes (addition of ions to or loss from mineral surface) are so rapid (Marini, 2006). Secondly, this may be due to a protective function of the biofilm where the presence of extracellular polymeric substances protects the $CaCO_3$ from dissolving. While mass transport limitations might be reduced in flowing systems due to

enhanced advection of reactants and products (Wang and Jaffe, 2004), the possible protective function of the biofilm would still reduce the degree of $CaCO_3$ dissolution. In biofilm-affected systems, the dissolution might be slowed down significantly due to diffusion limitations (Stewart, 2003) and mineral dissolution has been described to be affected by polysaccharides (Banfield et al., 1999). The close association of *S. pasteurii* biofilms and microbially precipitated $CaCO_3$ minerals has been demonstrated by us previously (Schultz et al., 2011). These data demonstrate that in high pressure brines, microbially enhanced $CaCO_3$ precipitates will likely be most stable in the long term in the $scCO_2$ region and in the $scCO_2$ saturated brine region where advection is limited. GCS site geology, specifically the abundance of silisiclastic or carbonate bedrock will also have a major control on the in situ pH and the saturation of $CaCO_3$ minerals both before and after $scCO_2$ injection which may impact the effectiveness of microbially induced mineralization and pore plugging. Specifically, pH and $CaCO_3$ saturation will be higher and pH and oversaturation will be maintained in the long-term more readily in pore spaces in carbonate bedrock than silisiclastic bedrock sites, from the dissolution and buffering of the native carbonate minerals (Carey et al., 2010; Kaszuba and Janecky, 2009; Kaszuba et al., 2003, 2005). This will enhance the stability of the microbially produced mineral plugs.

5. Conclusions

Experiments using a novel high pressure (~7.5 MPa) moderate temperature (32 °C) pulse-flow reactor containing a synthetic porous media core allowed microbiologically induced mineralization to be investigated under conditions approximating those in subsurface carbon storage environments. A surface-associated *S. pasteurii* biofilm became well established in the synthetic porous media core, which was able to hydrolyse all of the urea available in the daily media pulses at pressures of ~7.5 MPa. This raised the pH from 7 to 9.1, consistent with buffering by $NH_4^+ = NH_3 + H^+$ which has a pKa value of 9.3 at 30 °C and induced $CaCO_3$ precipitation. $CaCO_3$ precipitated as calcite, and a decreasing crystal density gradient with distance into the core suggested crystal growth was limited by the mass transport of Ca^{2+} and urea. Challenges of precipitated $CaCO_3$ with brine/$scCO_2$ static mixtures for 2–48 h investigated the potential stability of the precipitates under conditions that approximated a range of pre- and post-CO_2 injection conditions. Brine at atmospheric conditions generated a slight mass loss, due to dissolution of the mineral phase. $scCO_2$ had a negligible effect on mass, but $scCO_2$ equilibrated brine generated a significant $CaCO_3$ mass loss. However, control experiments with acidified brine (pH 4, the estimated minimum in situ pH of the $scCO_2$ equilibrated brine) demonstrated that much of the mass loss in the $scCO_2$ equilibrated brine experiments was due to the physical agitation of the $CaCO_3$ crystals during depressurisation and degassing at the termination of the experiments. Mass loss was not due to acidic dissolution of the $CaCO_3$, which appeared to be limited due to the protective effect of the biofilm and the static incubation of the brine + $CaCO_3$ where reaction kinetics are reduced by the limited ability of reactants and products to migrate to and from the mineral surface by advection. These data suggest that microbially induced mineralization with the purpose of reducing the permeability of preferential leakage pathways during the operation of GCS are applicable in the $scCO_2$ region and both the $scCO_2$ saturated brine region and the brine saturated $scCO_2$ region of the subsurface storage site where subsurface fluids are quasi static.

New and novel tools to control subsurface permeability and CO_2 leakage, as presented here, are required in inaccessible subsurface environments, where 'traditional' engineering approaches cannot be applied. For example, while injection wells may be accessible to traditional sealing approaches, reducing permeability proximal to the well bore or in fracture zones far from the well requires new approaches. While the injection of a base into the subsurface could achieve a pH increase and induce $CaCO_3$ precipitation similarly to the ureolysis based approach, this would lead to instantaneous $CaCO_3$ supersaturation and precipitation at the point of injection. However, the controlled injection of urea into the subsurface would allow for transport of urea farther away from the injection point before urea hydrolysis induced pH increase and $CaCO_3$ precipitation would occur. This is likely to promote a wider spatial distribution of $CaCO_3$ and avoid uncontrolled plugging at the point of injection (Ferris et al., 2003; Mitchell and Ferris, 2005). The injection of ureolytic organisms could also enhance the precipitation process, particularly since bacterial cells can migrate through pore throat sizes in common GCS site rocks. Recent work has been up-scaled by investigating radial flow and ureolytic $CaCO_3$ precipitation at atmospheric pressures, within 74 cm diameter, 38 cm thick sandstone cores (Phillips et al., 2012) and ongoing work is focusing on up-scaling under pressures that approximate GCS conditions.

Acknowledgments

Funding was provided from the US Department of Energy (DOE) Zero Emissions Research Technology Center (ZERT), Award No. DE-FC26-04NT42262 and DOE EPSCoR Award No. DE-FG02-08ER46527, NSF Award No. 0934696, as well as a European Union (EU) Marie Curie Reintegration Grant to ACM (277005). Support for the Environmental and Biofilm Mass Spectrometry Facility through DURIP, Contract Number: W911NF0510255 and the MSU Thermal Biology Institute from the NASA Exobiology Program Project NAG5-8807 is acknowledged.

Appendix A. Supplementary data

Supplementary data associated with this article can be found, in the online version, at http://dx.doi.org/10.1016/j.ijggc.2013.02.001.

References

Abe, F., Kato, C., Horikoshi, K., 1999. Pressure-regulated metabolism in microorganisms. Trends in Microbiology 7, 447–453.
Allen, D.E., Strazisar, B.R., Soong, Y., Hedges, S.W., 2005. Modeling carbon dioxide sequestration in saline aquifers: significance of elevated pressures and salinities. Fuel Processing Technology 86, 1569–1580.
Banfield, J.F., Barker, W.W., Welch, S.A., Taunton, A., 1999. Biological impact on mineral dissolution: application of the lichen model to understanding mineral weathering in the rhizosphere. Proceedings of the National Academy of Sciences 96, 3404–3411.
Barkley, W., Richardson, J., 1994. Laboratory safety. In: Gerhardt, P., Murray, R., Wood, E., Willis, A., Krieg, N. (Eds.), Manual of Methods for General Bacteriology. American Society of Microbiology, Washington, DC, pp. 715–734.
Burne, R.A., Chen, Y.-Y.M., 2000. Bacterial ureases in infectious diseases. Microbes and Infection 2, 533–542.
Carey, W., Svec, R., Grigg, R., Zhang, J., Crow, W., 2010. Experimental investigation of wellbore integrity and CO_2-brine flow along the casing-cement microannulus. International Journal of Greenhouse Gas Control 4, 272–282.
Castanier, S., Le Métayer-Levrel, G., Perthuisot, J.-P., 1999. Ca-carbonates precipitation and limestone genesis – the microbiogeologist point of view. Sedimentary Geology 126, 9–23.
Costerton, J.W., Stewart, P.S., 2001. Battling biofilms – the war is against bacterial colonies that cause some of the most tenacious infections known. The weapon is knowledge of the enemy's communication system. Scientific American 285, 74–81.
Cunningham, A., Sharp, R., Hiebert, R., James, G., 2003. Subsurface biofilm barriers for the containment and remediation of contaminated groundwater. Bioremediation Journal 7, 151–164.
Cunningham, A.B., Gerlach, R., Spangler, L., Mitchell, A.C., 2009. Microbially enhanced geologic containment of sequestered supercritical CO_2. Energy Procedia 1, 3245–3252.

Cunningham, A.B., Gerlach, R., Spangler, L., Mitchell, A.C., Parks, S., Phillips, A., 2011. Reducing the risk of well bore leakage of CO_2 using engineered biomineralization barriers. Energy Procedia 4, 5178–5185.

Duan, Z., Sun, R., 2003. An improved model calculating CO_2 solubility in pure water and aqueous NaCl solutions from 273 to 533 K and from 0 to 2000 bar. Chemical Geology 193, 257–271.

Dupraz, S., Parmentier, M., Ménez, B., Guyot, F., 2009. Experimental and numerical modeling of bacterially induced pH increase and calcite precipitation in saline aquifers. Chemical Geology 265, 44–53.

Ferris, F.G., Stehmeier, L.G., Kantzas, A., Mourits, F.M., 1996. Bacteriogenic mineral plugging. Journal of Canadian Petroleum Technology 35, 56–61.

Ferris, F.G., Phoenix, V., Fujita, Y., Smith, R.W., 2003. Kinetics of calcite precipitation induced by ureolytic bacteria at 10 to 20 degrees C in artificial groundwater. Geochimica Et Cosmochimica Acta 68, 1701–1710.

Fujita, Y., Ferris, F.G., Lawson, R.D., Colwell, F.S., Smith, R.W., 2000. Calcium carbonate precipitation by ureolytic subsurface bacteria. Geomicrobiology Journal 17, 305–318.

Fujita, Y., Taylor, J.L., Gresham, T.L., Delwiche, M.E., Colwell, F.S., McLing, T., Petzke, L., Smith, R.W., 2008. Stimulation of microbial urea hydrolysis in groundwater to enhance calcite precipitation. Environmental Science & Technology 42, 3025–3032.

Gerlach, R., Cunningham, A.B., 2010. Influence of biofilms on porous media hydrodynamics. In: Vafai, K. (Ed.), Porous Media: Applications in Biological Systems and Biotechnology. Taylor Francis, Boca Raton London New York, pp. 173–230.

Gledhill, D.K., Morse, J.W., 2004. Dissolution kinetics of calcite in $NaCl–CaCl_2–MgCl_2$ brines at 25 degrees C and 1 bar pCO_2. Aquatic Geochemistry 10, 171–190.

Gledhill, D.K., Morse, J.W., 2006. Calcite dissolution kinetics in Na–Ca–Mg–Cl brines. Geochimica Et Cosmochimica Acta 70, 5802–5813.

Gómez-Morales, J., Torrent-Burgués, J., Rodríguez-Clemente, R., 1996. Nucleation of calcium carbonate at different initial pH conditions. Journal of Crystal Growth 169, 331–338.

Gross, M., Lehle, K., Jaenicke, R., Nierhaus, K.H., 1993. Pressure-induced dissociation of ribosomes and elongation cycle intermediates – stabilizing conditions and identification of the most sensitive functional-state. European Journal of Biochemistry 218, 463–468.

Hammes, F., Seka, A., de Kniff, S., Verstraete, W., 2003. A novel approach to calcium removal from calcium-rich industrial wastewater. Water Research 37, 699–704.

Hansen, L., 2009. Design and experimental testing of a high pressure, high temperature flow-through rock core reactor using supercritical carbon dioxide. M.S. Thesis, Montana State University.

Harkes, M.P., van Paassen, L.A., Booster, J.L., Whiffin, V.S., van Loosdrecht, M.C.M., 2010. Fixation and distribution of bacterial activity in sand to induce carbonate precipitation for ground reinforcement. Ecological Engineering 36, 112–117.

Jenneman, G.E., McInerney, M.J., Knapp, R.M., 1985. Microbial penetration through nutrient-saturated berea sandstone. Applied and Environment Microbiology 50, 383–391.

Kaszuba, J.P., Janecky, D.R., 2009. Geochemical impacts of sequestering carbon dioxide in brine aquifers. In: McPherson, J.M., Sundquist, E. (Eds.), Carbon Sequestration and its Role in the Global Carbon Cycle, Volume 183. American Geophysical Union Monograph, Washington, DC, pp. 239–247.

Kaszuba, J.P., Janecky, D.R., Snow, M.G., 2003. Carbon dioxide reaction processes in a model brine aquifer at 200 degrees C and 200 bars: implications for geologic sequestration of carbon. Applied Geochemistry 18, 1065–1080.

Kaszuba, J.P., Janecky, D.R., Snow, M.G., 2005. Experimental evaluation of mixed fluid reactions between supercritical carbon dioxide and NaCl brine: relevance to the integrity of a geologic carbon repository. Chemical Geology 217, 277–293.

Lagneau, V., Pipart, A., Catalette, H., 2005. Modélisation couplée chimie-transport du comportement à long terme de la séquestration géologique de CO_2 dans des aquifères salins profonds. Oil & Gas Science and Technology – RelFP 60, 231–247.

Lewandowski, Z., Beyenal, H., 2007. Fundamentals of Biofilm Research. CRC Press, London, p. 452.

Marini, L., 2006. The kinetics of mineral carbonation. In: Marini, L. (Ed.), Developments in Geochemistry, Vol. 11. Elsevier, Chapter 6, pp. 169–317.

Mitchell, J., Carlos Santamarina, J., 2004. Biological considerations in geotechnical engineering. Journal of Geotechnical & Geoenvironmental Engineering 131, 1222–1233.

Mitchell, A.C., Ferris, F.G., 2005. The co-precipitation of sr into calcite precipitates induced by bacterial ureolysis in artificial groundwater – temperature and kinetic dependence. Geochimica Et Cosmochimica Acta 69, 4199–4210.

Mitchell, A.C., Ferris, F.G., 2006a. Effect of strontium contaminants upon the size and solubility of calcite crystals precipitated by the bacterial hydrolysis of urea. Environmental Science & Technology 40, 1008–1014.

Mitchell, A.C., Ferris, F.G., 2006b. The influence of *Bacillus pasteurii* on the nucleation and growth of calcium carbonate. Geomicrobiology Journal 23, 213–226.

Mitchell, A.C., Phillips, A.J., Hamilton, M.A., Gerlach, R., Hollis, W.K., Kaszuba, J.P., Cunningham, A.B., 2008. Resilience of planktonic and biofilm cultures to supercritical CO_2. Journal of Supercritical Fluids 47, 318–325.

Mitchell, A.C., Phillips, A., Hiebert, R., Gerlach, R., Spangler, L., Cunningham, A.B., 2009. Biofilm enhanced subsurface sequestration of supercritical CO_2. The International Journal on Greenhouse Gas Control 3, 90–99.

Mitchell, A.C., Dideriksen, K., Spangler, L.H., Cunningham, A.B., Gerlach, R., 2010. Microbially enhanced carbon capture and storage by mineral-trapping and solubility-trapping. Environmental Science & Technology 44, 5270–5276.

Murray, J.W., Emerson, S., Jahnke, R., 1980. Carbonate saturation and the effect of pressure on the alkalinity of interstitial waters from the Guatemala Basin. Geochimica Et Cosmochimica Acta 44, 963–972.

Nelson, P.H., 2009. Pore-throat sizes in sandstones, tight sandstones, and shales. AAPG Bulletin 93, 329–340.

Nicot, J.-P., Oldenburg, C.M., Bryant, S.L., Hovorka, S.D., 2009. Pressure perturbations from geologic carbon sequestration: area-of-review boundaries and borehole leakage driving forces. Energy Procedia 1, 47–54.

Pan, L., Oldenburg, C.M., Wu, Y.-S., Pruess, K., 2009. Wellbore flow model for carbon dioxide and brine. Energy Procedia 1, 71–78.

Parkhust, D., Appelo, C., 1999. User's guide to PHREEQC (Version 2) – a computer program for speciation, batch-reaction, one-dimensional transport, and inverse geochemical calculations. U.S. Geological Survey, Water-Resources Investigations Report 99-4259, p. 312.

Phillips, A.J., Lauchnor, E., Eldring, J., Esposito, R., Mitchell, A.C., Gerlach, R., Cunningham, A.B., Spangler, L.H., 2012. Potential CO_2 leakage reduction through biofilm-induced calcium carbonate precipitation. Environmental Science & Technology 47, 142–149.

Pytkowicz, R.M., Conners, D.N., 1964. High pressure solubility of calcium carbonate in seawater. Science 144, 840–841.

Sanz, E., Ayora, C., Carrera, J., 2011. Calcite dissolution by mixing waters: geochemical modeling and flow-through experiments. Geologica Acta 9, 67–77.

Schultz, L., Pitts, B., Mitchell, A.C., Cunningham, A.B., Gerlach, R., 2011. Imaging biologically-induced mineralization in fully hydrated flow systems. Microscopy Today 2011 (September), 12–15.

Schultze-Lam, S., Fortin, D., Davis, B.S., Beveridge, T.J., 1996. Mineralization of bacterial surfaces. Chemical Geology 132, 171–181.

Stewart, P.S., 2003. Diffusion in biofilms. Journal of Bacteriology 185, 1485–1491.

Stumm, W., Morgan, J.J., 1996. Aquatic Chemistry. John Wiley & Sons, New York, 1040 p.

Teng, H.H., Dove, P.M., De Yoreo, J.J., 2000. Kinetics of calcite growth: surface processes and relationships to macroscopic rate laws. Geochimica Et Cosmochimica Acta 64, 2255–2266.

Van Lith, Y., Warthmann, R., Vasconcelos, C., McKenzie, J.A., 2003. Microbial fossilization in carbonate sediments: a result of the bacterial surface involvement in dolomite precipitation. Sedimentology 50, 237–245.

Van Paassen, L.A., Daza, C.M., Staal, M., Sorokin, D.Y., van der Zon, W., van Loosdrecht, M.C.M., 2010a. Potential soil reinforcement by biological denitrification. Ecological Engineering 36, 168–175.

Van Paassen, L.A., Ghose, R., Van der Linden, T., Van der Star, W., Van Loosdrecht, M., 2010b. Quantifying biomediated ground improvement by ureolysis: large-scale biogrout experiment. Journal of Geotechnical and Geoenvironmental Engineering 136, 1721–1728.

Wang, S., Jaffe, P.R., 2004. Dissolution of a mineral phase in potable aquifers due to CO_2 releases from deep formations; effect of dissolution kinetics. Energy Conversion and Management 45, 2833–2848.

Warren, L.A., Maurice, P.A., Parmar, N., Ferris, F.G., 2001. Microbially mediated calcium carbonate precipitation: implications for interpreting calcite precipitation and for solid-phase capture of inorganic contaminants. Geomicrobiology Journal 18, 93–115.

Whiffin, V.S., van Paassen, L.A., Harkes, M.P., 2007. Microbial carbonate precipitation as a soil improvement technique. Geomicrobiology Journal 24, 417–423.

White, C.M., Strazisar, B.R., Granite, E.J., Hoffman, J.S., Pennline, H.W., 2003. Separation and capture of CO_2 from large stationary sources and sequestration in geological formations – coalbeds and deep saline aquifers. Journal of the Air & Waste Management Association 53, 645–715.

Yayanos, A.A., Pollard, E.C., 1969. A study of effects of hydrostatic pressure on macromolecular synthesis in *Escherichia coli*. Biophysical Journal 9, 1464.

Zakkour, P., Haines, M., 2007. Permitting issues for CO_2 capture, transport and geological storage: a review of Europe USA, Canada and Australia. International Journal of Greenhouse Gas Control 1, 94–100.

Zhang, T., Klapper, I., 2010. Mathematical model of biofilm induced calcite precipitation. Water Science & Technology 61, 2957–2964.